FEBS Letters 453 (1999) 164–168 FEBS 22169

# Di-, tri- and tetrameric single chain Fv antibody fragments against human CD19: effect of valency on cell binding

Fabrice Le Gall[a,b,1], Sergey M. Kipriyanov[a,1], Gerhard Moldenhauer[b], Melvyn Little[a,*]

[a] *Recombinant Antibody Research Group (D0500), German Cancer Research Center (DKFZ), Im Neuenheimer Feld 280, D-69120 Heidelberg, Germany*

[b] *Department of Molecular Immunology, DKFZ, Im Neuenheimer Feld 280, D-69120 Heidelberg, Germany*

Received 10 May 1999

**Abstract Single chain variable fragments (scFv) of the murine monoclonal antibody HD37 specific to human B-cell antigen CD19 were constructed by joining the $V_H$ and $V_L$ domains with linkers of 18, 10, 1 and 0 residues. ScFv-18 formed monomers, dimers and small amounts of tetramers; scFv-10 formed dimers and small amounts of tetramers; scFv-1 formed exclusively tetramers; scFv-0 formed exclusively trimers. The affinities of the scFv-10 (diabody) and scFv-1 (tetrabody) were approximately 1.5- and 2.5-fold higher, respectively, than that of the scFv-0 (triabody). The tetrabody displayed a significantly prolonged association with cell-bound antigen ($t_{1/2}$ cell surface retention at 37°C of 26.6 min) compared to both the diabody (13.3 min) and triabody (6.7 min). This increase in avidity of the tetrabody combined with its larger size could prove to be particularly advantageous for imaging and the immunotherapy of B-cell malignancies.**



*Key words:* Single chain Fv; Diabody; Triabody; Tetrabody; Human CD19

## 1. Introduction

A major goal of antibody-based tumor targeting has been to specifically deliver a variety of agents such as radioisotopes, drugs, toxins, lymphokines, and enzymes for imaging and therapy. Intact IgG molecules are large (150 kDa) glycoproteins that exhibit a slow systemic clearance, often leading to poor tumor targeting specificity. Smaller antibody-derived molecules include enzymatically produced 50 kDa Fab fragments and engineered 25 kDa single chain Fv (scFv) consisting of the heavy and light chain variable regions ($V_H$ and $V_L$) connected by a flexible 14–24 amino acid long peptide linker [1,2]. Compared to IgG molecules, Fab and scFv exhibit significantly improved tumor specificity and intratumoral penetration [3–5]. However, the rapid blood clearance and monovalent nature of these small molecules result in significantly lower quantitative tumor retention of scFv and Fab fragments [3,6].

Recently, attention has focused upon the generation of scFv-based molecules with molecular weights in the range of the renal threshold for first pass clearance. Construction of such molecules can be achieved by shortening the linker between the $V_H$ and $V_L$ domains in scFv. Reduction of the linker length to shorter than 12 residues prevents the monomeric configuration of the scFv molecule and favors intermolecular $V_H$-$V_L$ pairings with formation of a 50 kDa non-covalent scFv dimer 'diabody' [7,8]. Prolonged tumor retention in vivo and higher tumor to blood ratios reported for diabodies over scFv monomers result both from the reduced kidney clearance and higher avidity [9,10]. ScFv molecules constructed by direct fusion of the C-terminal residue of $V_H$ to N-terminal residue of $V_L$ (i.e. without any linker sequence) can form a trimer 'triabody' with a molecular mass of 75–80 kDa and three antigen binding sites [8,11].

We recently described the construction and characterization of an scFv antibody fragment specific for the human B-cell antigen CD19 [12]. The CD19 antigen is expressed on virtually all B-lineage malignancies from acute lymphoblastic leukemia (ALL) to non-Hodgkin's lymphoma (NHL) [13]. Moreover, it is not shed and is absent from hemopoietic stem cells, plasma cells, T-cells and other tissues. CD19 is therefore one of the best targets for immunotherapy of B-cell malignancies. In order to develop an effective means for the delivery of radionuclides to a tumor site, we constructed a set of anti-CD19 scFv fragments, in the present study, with a linker comprising 0, 1 and 10 residues. We observed the quantitative formation of diabodies by scFv-10 and triabodies by scFv-0. Anti-CD19 scFv with a linker of one amino acid residue formed exclusively 'tetrabodies'. A comparison of the in vitro binding characteristics of the diabody, triabody and tetrabody to $CD19^+$ cells demonstrated some surprising differences.

## 2. Materials and methods

### 2.1. Vector constructions

The plasmid pHOG21-αCD19 encoding an scFv fragment with an 18 amino acid linker (scFv-18) specific for human CD19 [12] was used as a material for all of the constructs. To create anti-CD19 scFv-10, a $V_H$ gene was cut with *Nco*I/*Hin*dIII from the plasmid pHOG21-αCD19 and recloned into the *Nco*I/*Hin*dIII linearized vector pHOG3-19 originally encoding the hybrid $V_H$3-$V_L$19 scFv [14]. For the construction of genes encoding scFv-0 and scFv-1, the PCR fragments of the $V_H$ domain of anti-CD19 were generated using the primers DP1, 5′-TCA CAC AGA ATT CTT AGA TCT ATT AAA GAG GAG AAA TTA ACC and either $V_H$/S, 5′-GAG CAA GAT ATC GGA GAC GGT GAC TGA GGT TCC, or $V_H$/SS, 5′-GAG CAA GAT ATC TGA GGA GAC GGT GAC TGA GGT TCC, respectively. The resulting PCR fragments were digested with *Nco*I and *Eco*RV and ligated with the *Nco*I/*Eco*RV linearized plasmid pHOG-αCD19. All sequences encoding scFv fragments were verified by the dideoxynucleotide method [15].

### 2.2. Protein expression and purification

For expression of scFv fragments, the plasmids were transformed into *Escherichia coli* K12 strain XL1-Blue (Stratagene, La Jolla, CA, USA). Transformed bacteria were grown at 37°C in shake flasks containing 2×YT medium with 0.1 g/l ampicillin and 100 mM glucose. IPTG induction and isolation of periplasmic extracts were performed

*Corresponding author. Fax: +49 (6221) 423462.
E-mail: m.little@dkfz-heidelberg.de

[1] These authors made equal contributions to this work.


PII: S0014-5793(99)00713-9

as previously described [16,17]. For isolation of scFv fragments, the culture supernatant and the soluble periplasmic extract were combined and concentrated using Amicon YM10 membranes with a 10 kDa cut-off (Amicon, Witten, Germany) followed by thorough dialysis against 50 mM Tris-HCl, 1 M NaCl, pH 7.0. Purification was achieved by immobilized metal affinity chromatography (IMAC) using a $Cu^{2+}$-charged Chelating Sepharose (Pharmacia, Freiburg, Germany), as described [17]. The final purification was achieved by ion-exchange chromatography on a MonoQ HR5/5 column (Pharmacia) in 20 mM Tris-HCl, pH 8.0 with a linear 0–1 M NaCl gradient. All purification procedures were performed at 4°C.

The bispecific CD3×CD19 diabody was isolated as previously described [14].

### 2.3. SDS-PAGE and size-exclusion chromatography

SDS-PAGE was performed according to Laemmli [18] under reducing conditions. Analytical gel filtration of the scFv preparations was performed on a calibrated Superdex 200 HR10/30 column (Pharmacia) in PBSI (15 mM Na-phosphate, 0.15 M NaCl, 50 mM imidazole, pH 7.0). Sample volume and flow rate were 50 μl and 0.5 ml/min, respectively.

### 2.4. Flow cytometry and affinity determination

The human $CD19^+$ B-cell line JOK-1 was used for flow cytometry as previously described [14]. The apparent affinities of recombinant antibody molecules were determined from competitive inhibition assays [14]. Briefly, increasing concentrations of purified antibody fragment were added to a subsaturating concentration of FITC-labeled mAb HD37 (anti-CD19) and were incubated with JOK-1 cells. Fluorescence intensities of stained cells were measured using a FACScan flow cytometer (Becton Dickinson, Mountain View, CA, USA). Binding affinities were calculated according to the following equation: $K_{D(I)} = IC_{50}/(1+[\text{FITC-mAb}]/K_{D(mAb)})$, where $I$ is the unlabeled inhibitor (diabody, triabody or tetrabody), [FITC-mAb] is the concentration of FITC-labeled mAb HD37, $K_{D(mAb)}$ is the binding affinity of mAb and $IC_{50}$ is the concentration of inhibitor that yields 50% inhibition of binding. An affinity constant ($K_D$) value of 0.4 nM was assigned to mAb HD37 [14].

### 2.5. Cell surface retention assay

In vitro cell surface retention assays were performed at 37°C essentially as described [10] except that the detection of the retained antibody fragments was performed using anti-c-*myc* mAb 9E10 (IC Chemikalien, Ismaning, Germany) followed by FITC-labeled anti-mouse IgG. Kinetic dissociation constants ($k_{off}$) were calculated using a first order equation $F_t = F_0 \times e^{-kt}$, where $F_t$ is fluorescence at time $t$, $F_0$ is fluorescence at time 0 and $k$ is $k_{off}$. The half-life ($t_{1/2}$) for dissociation of antibody fragments was calculated from the equation $t_{1/2} = \ln 2/k_{off}$.

## 3. Results

### 3.1. ScFv construction, expression and purification

The anti-CD19 scFv gene construct [12], in which the $V_H$ and $V_L$ domains were linked with the 18 residue YOL linker (scFv-18), was used as a template to create new oligomeric scFv species (Fig. 1a). ScFv-10 was constructed using a 10 amino acid linker mainly comprising N-terminal residues from the $C_{H1}$ domain that has been successfully used previously for making a bispecific CD3×CD19 diabody [14]. The other two scFv genes were constructed by ligating the codon for C-terminal $V_H$-$Ser^{112}$ with N-terminal $V_L$-$Asp^1$ for scFv-0 and C-terminal $V_H$-$Ser^{113}$ with N-terminal $V_L$-$Asp^1$ for scFv-1 (numeration is given according to Kabat et al. [19]). All scFv fragments were produced in *E. coli* by secretion into the bacterial periplasm. The soluble antibody fragments were isolated from periplasmic extracts and culture medium by two chromatographic steps with typical yields of 0.8–1.0 mg per 1 l of shake flask culture and with a purity greater than 95% (Fig. 2).

### 3.2. Protein analysis

Gel filtration on a calibrated Superdex 200 column demonstrated that the scFv-18 protein was distributed between three peaks with apparent molecular masses of 29 (40% of total material), 56 (55%) and 115 kDa (5%), corresponding to scFv monomer, dimer and tetramer, respectively (Fig. 3a). In contrast, scFv-10 appeared to be predominantly dimeric (diabody) with only a small proportion of tetramers (Fig. 3b). Size-exclusion chromatography of both scFv-1 and scFv-0 yielded single symmetrical peaks with apparent molecular masses of 115 (tetramer) and 87 kDa (trimer), respectively (Fig. 3c, d).

Flow cytometry experiments demonstrated a specific interaction of all the scFv fragments with $CD19^+$ JOK-1 cells. The fluorescence intensities obtained for scFv-1 (tetrabody) were somewhat higher than those for scFv-0 (triabody) and scFv-10 (diabody) over a wide range of protein concentrations (Fig. 4a). Similarly, the signals for scFv-0 were somewhat higher than those for scFv-10. These differences might result from a

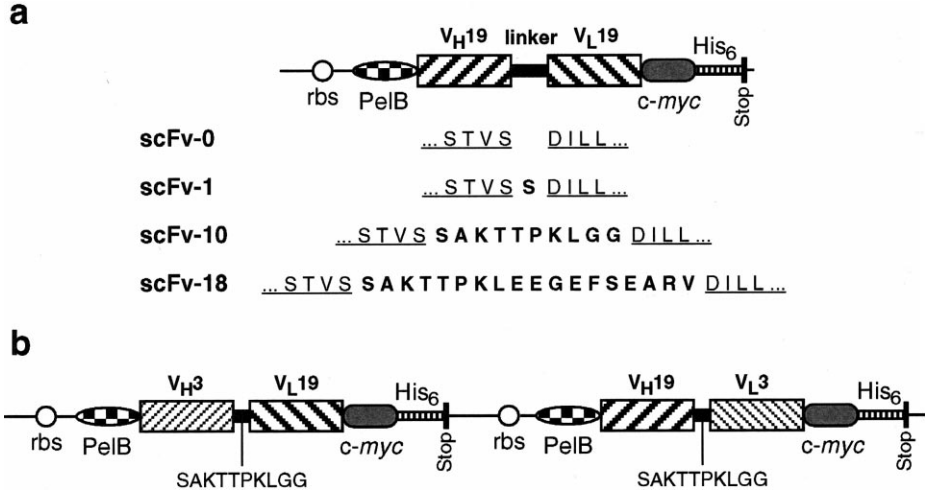


Fig. 1. Expression cassettes for anti-CD19 scFv constructs. a: Monospecific constructs with various linker peptides. C-terminal sequences of $V_H$ and N-terminal sequences of $V_L$ are underlined. The linker peptide is shown in bold. b: CD3×CD19 diabody. The sequences of linkers are shown below the diagram. The locations of ribosome binding site (rbs), *pel*B leader (pelB), c-*myc* epitope (c-*myc*), hexahistidine tag ($his_6$) and stop codon (Stop) are indicated.

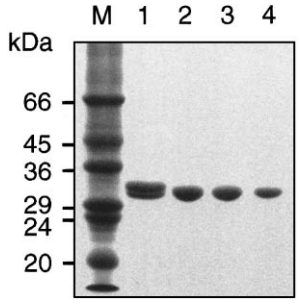


Fig. 2. Reducing SDS-PAGE of purified antibody fragments. Lanes: M, MW markers; 1, bispecific CD3×CD19 diabody; 2, scFv-10; 3, scFv-0; 4, scFv-1. The gel was stained with Coomassie brilliant blue.

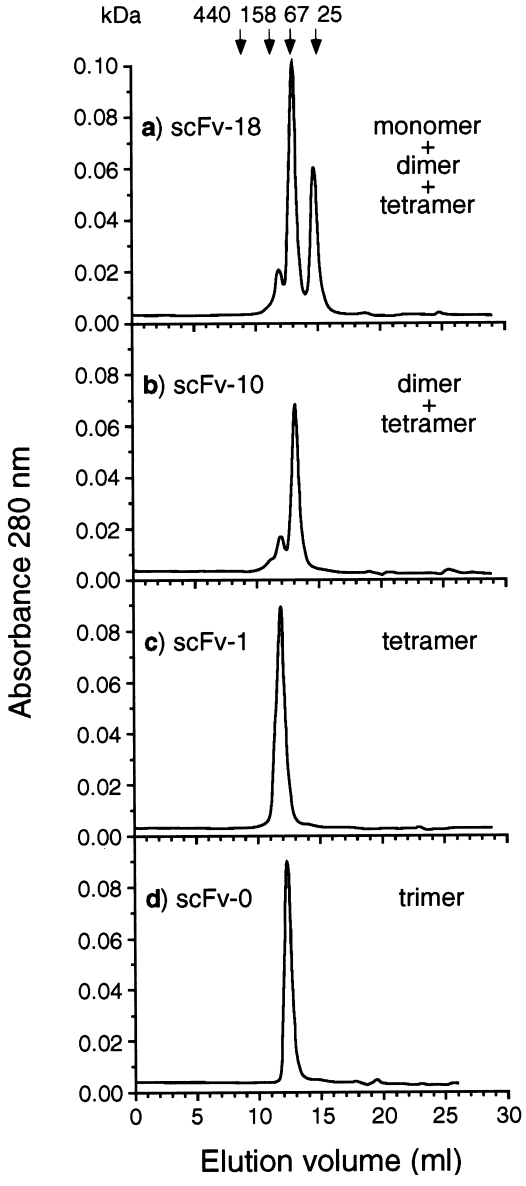


Fig. 3. Size-exclusion FPLC of anti-CD19 antibody fragments on a calibrated Superdex 200 HR10/30 column. a: scFv-18, b: scFv-10, c: scFv-1 and d: scFv-0.

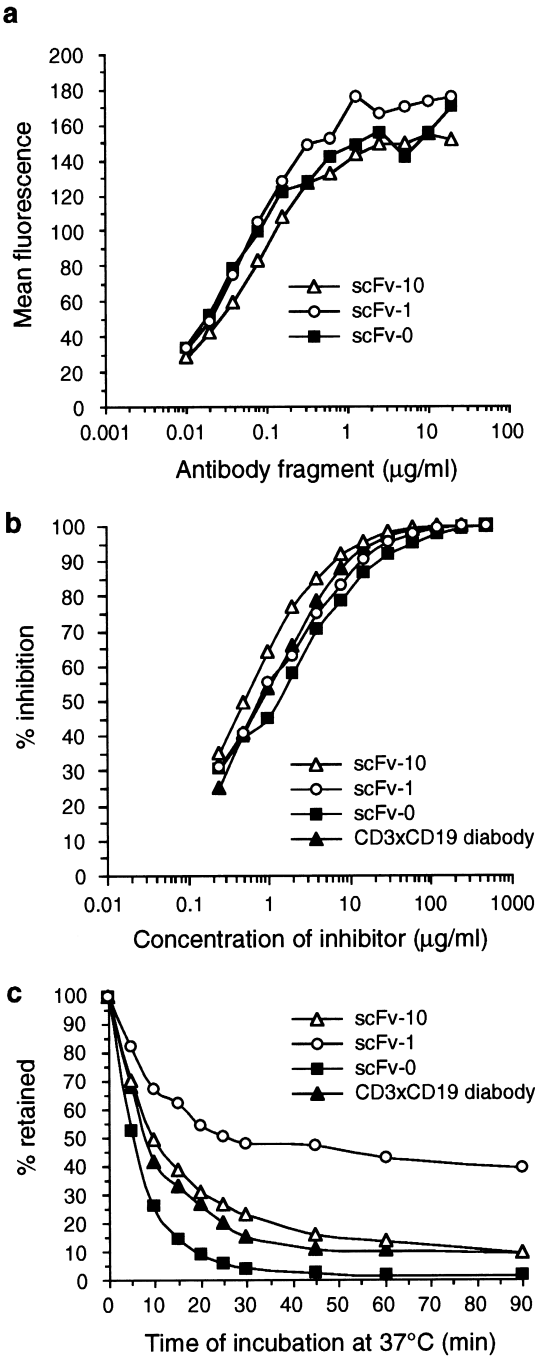


Fig. 4. Analyses of antigen binding activities of antibody fragments. a: Direct binding to CD19$^+$ JOK-1 cells as determined by flow cytometry. b: Inhibition of binding of FITC-labeled mAb HD37 to JOK-1 cells. c: Cell surface retention in vitro at 37°C.

gain in affinity through avidity that could be expected for trimeric or tetrameric molecules but they could also reflect the number of c-*myc* epitopes used for the immunodetection of each scFv oligomer. We therefore analyzed the apparent affinities of the scFv fragments by competitive binding to human JOK-1 cells in the presence of FITC-labeled anti-CD19 mAb HD37 (Fig. 4b). The relative affinities were calculated from the corresponding $IC_{50}$ values. Due to the presence of different molecular forms in scFv-18 preparations (Fig. 3a), instead of the parental scFv monomer we used the well char-

Table 1
Affinity and binding kinetics of anti-human CD19 antibody fragments

| Antibody | $IC^a_{50}$ (μg/ml) | $IC^a_{50}$ (nM) | $K^a_D$ (nM) | $k^b_{off}$ ($s^{-1}/10^{-4}$) | $t^b_{1/2}$ (min) |
|---|---|---|---|---|---|
| CD3×CD19 diabody | 0.83 | 14.3 | 0.73 | 10.95 ± 2.60 | 10.6 |
| scFv-10 (diabody) | 0.50 | 8.5 | 0.44 | 8.67 ± 2.67 | 13.3 |
| scFv-1 (tetrabody) | 0.74 | 6.5 | 0.33 | 4.33 ± 1.76 | 26.6 |
| scFv-0 (triabody) | 1.25 | 14.6 | 0.75 | 17.33 ± 5.16 | 6.7 |

[a]Deduced from inhibition experiments.
[b]Deduced from cell surface retention assays.

acterized bispecific CD3×CD19 diabody [14] as an example of monovalent binding to a $CD19^+$ cell surface. The bispecific diabody comprising two hybrid scFv fragments ($V_H$3-$V_L$19 and $V_H$19-$V_L$3) was purified to homogeneity (Fig. 2, lane 1) and appeared upon gel filtration as a single peak with a molecular mass of 50–55 kDa (data not shown). Results of inhibition experiments demonstrated that scFv-0 (triabody) bound CD19 with an affinity almost identical to that of the CD3×CD19 diabody, whereas scFv-10 (diabody) and scFv-1 (tetrabody) demonstrated approximately 1.5- and 2.5-fold increases in affinity, respectively (Table 1).

To investigate the biological relevance of the differences in affinity values of the scFv fragments, their in vitro retention on the surface of CD19-positive cells incubated at 37°C was determined by flow cytometry (Fig. 4c). The scFv-10 (diabody) had a relatively short retention half-life ($t_{1/2}$) on $CD19^+$ cells, almost identical to the $t_{1/2}$ of the bispecific diabody (Table 1). In contrast, scFv-1 (tetrabody) was retained 2.5-fold longer than the bispecific diabody. Surprisingly, scFv-0 (triabody) demonstrated the shortest half-life, suggesting that only one antigen binding site of this trimer interacts with the cell surface (Fig. 4c, Table 1).

## 4. Discussion

The design of linker length in this study was based on the observation that shortening the distance between $V_H$ and $V_L$ domains in scFv below 12 residues forces an intermolecular pairing of domains into dimers, termed diabodies [7,8]. Direct fusion of $V_H$ and $V_L$ domains without any linker has been shown to further constrain the domain association, resulting in trimers, termed triabodies [8,11,20]. The C-terminal residue in the $V_H$ domain of the triabodies was either $Ser^{112}$ [8] or $Ser^{113}$ [11,20]. Even one additional amino acid between the $V_H$ and $V_L$ domains was enough to provide the extra flexibility required for the formation of a diabody instead of a triabody.

To obtain higher valency constructs for the HD37 anti-CD19 scFv, we constructed two zero linker scFv fragments with and without $Ser^{113}$ residue at the $V_H$-$V_L$ junction, named scFv-1 and scFv-0, respectively. As expected, scFv-10 formed mainly dimers and scFv-0 formed only trimers (Fig. 3b, d). Both were shown to bind CD19 by flow cytometry. In contrast to previously described scFv fragments containing the $V_H$ domain linked to $V_L$ via $Ser^{113}$ that formed either dimers [7] or trimers [11,20], our scFv-1 exclusively formed tetrameric molecules with apparent molecular mass of 115 kDa (Fig. 3c). The tetramerization of such scFv antibody fragments with one residue linker is described here for the first time. Since our HD37 scFv effectively forms dimers even with a linker of 18 residues (Fig. 3a), the observed tetramerization might be dependent on the particular antibody fragment and its folding history [21].

Multiple binding to surface-bound antigens is dependent on both the correct orientation of $V_H$-$V_L$ pairs in a multivalent antibody complex and on epitope accessibility. Surprisingly, triabodies demonstrated the worst antigen binding characteristics among the examined scFv fragments. These results suggest that the anti-CD19 triabody can only bind monovalently to its cell surface anchored antigen. Inhibition experiments demonstrated an increase in affinity for scFv-10 (diabody) and scFv-1 (tetrabody) (Fig. 4b, Table 1), but only the tetrabody had a significantly lower dissociation rate compared to a monovalent binder (bispecific diabody) from the cell surface (Fig. 4c, Table 1). Although the tetrabody has four potentially active antigen binding sites, only two of them seem to be involved in binding cell anchored CD19. This conclusion comes from the similarity of retention half-lives for the anti-CD19 tetrabody (26.6 min, this study) and a recently constructed bispecific CD3×CD19 tandem diabody which has two CD19 binding sites (24.3 min, Kipriyanov et al., manuscript submitted).

The solution of the crystal structure of a diabody [22] showed that the $V_H$ domain of one chain is paired with $V_L$ domain of the other chain and vice versa. The triabody has three Fv heads with the polypeptides arranged in a cyclic, head-to-tail fashion [20]. It is tempting to speculate that the tetrabody described here has similar domain arrangement with a symmetric tetrameric conformation and less sterical constraints than the triabody. Rough estimations indicate that diagonal Fv modules in a square tetrabody can span distances up to 100 Å, significantly higher than distances between antigen binding sites in diabodies (65 Å [22]) and triabodies (75 Å [20]). Tetrabodies with their molecular mass of 115 kDa easily exceed the renal threshold for first pass elimination and should, therefore, exhibit significantly prolonged pharmacokinetics in comparison with scFv monomers and dimers. Tetrabodies might therefore be very useful molecules for tumor imaging and therapy.

*Acknowledgements:* This work was supported in part by a grant from the European Commission (BIO4 CT 972005).

## References

[1] Bird, R.E., Hardman, K.D., Jacobson, J.W., Johnson, S., Kaufman, B.M., Lee, S.-M., Lee, T., Pope, S.H., Riordan, G.S. and Whitlow, M. (1988) Science 242, 423–426.
[2] Huston, J.S., Huston, J.S., Levinson, D., Mudgett Hunter, M., Tai, M.S., Novotny, J., Margolies, M.N., Ridge, R.J., Bruccoleri, R.E., Haber, E., Crea, R. and Oppermann, H. (1988) Proc. Natl. Acad. Sci. USA 85, 5879–5883.
[3] Milenic, D.E., Yokota, T., Filpula, D.R., Finkelman, M.A., Dodd, S.W., Wood, J.F., Whitlow, M., Snoy, P. and Schlom, J. (1991) Cancer Res. 51, 6363–6371.
[4] Yokota, T., Milenic, D.E., Whitlow, M. and Schlom, J. (1992) Cancer Res. 52, 3402–3408.

[5] Yokota, T., Milenic, D.E., Whitlow, M., Wood, J.F., Hubert, S.L. and Schlom, J. (1993) Cancer Res. 53, 3776–3783.
[6] Adams, G.P., McCartney, J.E., Tai, M.S., Oppermann, H., Huston, J.S., Stafford, W.F., Bookman, M.A., Fand, I., Houston, L.L. and Weiner, L.M. (1993) Cancer Res. 53, 4026–4034.
[7] Holliger, P., Prospero, T. and Winter, G. (1993) Proc. Natl. Acad. Sci. USA 90, 6444–6448.
[8] Kortt, A.A., Lah, M., Oddie, G.W., Gruen, C.L., Burns, J.E., Pearce, L.A., Atwell, J.L., McCoy, A.J., Howlett, G.J., Metzger, D.W., Webster, R.G. and Hudson, P.J. (1997) Protein Eng. 10, 423–433.
[9] Wu, A.M., Chen, W., Raubitschek, A., Williams, L.E., Neumaier, M., Fischer, R., Hu, S.Z., Odom Maryon, T., Wong, J.Y. and Shively, J.E. (1996) Immunotechnology 2, 21–36.
[10] Adams, G.P., Schier, R., McCall, A.M., Crawford, R.S., Wolf, E.J., Weiner, L.M. and Marks, J.D. (1998) Br. J. Cancer 77, 1405–1412.
[11] Iliades, P., Kortt, A.A. and Hudson, P.J. (1997) FEBS Lett. 409, 437–441.
[12] Kipriyanov, S.M., Kupriyanova, O.A., Little, M. and Moldenhauer, G. (1996) J. Immunol. Methods 196, 51–62.
[13] Uckun, F.M. and Ledbetter, J.A. (1988) Proc. Natl. Acad. Sci. USA 85, 8603–8607.
[14] Kipriyanov, S.M., Moldenhauer, G., Strauss, G. and Little, M. (1998) Int. J. Cancer 77, 763–772.
[15] Sanger, F., Nicklen, S. and Coulson, A.R. (1977) Proc. Natl. Acad. Sci. USA 74, 5463–5467.
[16] Kipriyanov, S.M., Moldenhauer, G. and Little, M. (1997) J. Immunol. Methods 200, 69–77.
[17] Kipriyanov, S.M., Moldenhauer, G., Martin, A.C., Kupriyanova, O.A. and Little, M. (1997) Protein Eng. 10, 445–453.
[18] Laemmli, U.K. (1970) Nature 227, 680–685.
[19] Kabat, E.A., Wu, T.T., Perry, H.M., Gottesmann, K.S. and Foeller, C. (1991) Public Health Service, National Institutes of Health, Bethesda, MD.
[20] Pei, X.Y., Holliger, P., Murzin, A.G. and Williams, R.L. (1997) Proc. Natl. Acad. Sci. USA 94, 9637–9642.
[21] Arndt, K.M., Müller, K.M. and Plückthun, A. (1998) Biochemistry 37, 12918–12926.
[22] Perisic, O., Webb, P.A., Holliger, P., Winter, G. and Williams, R.L. (1994) Structure 2, 1217–1226.